JOURNAL OF VIROLOGY, Sept. 2009, p. 9258–9272 Vol. 83, No. 18
0022-538X/09/$08.00+0 doi:10.1128/JVI.00355-09

Protective and Pathologic Roles of the Immune Response to Mouse Hepatitis Virus Type 1: Implications for Severe Acute Respiratory Syndrome[▽]

Aaruni Khanolkar,[1]† Stacey M. Hartwig,[1]† Brayton A. Haag,[2] David K. Meyerholz,[3] Lecia L. Epping,[1] Jodie S. Haring,[1]‡ Steven M. Varga,[1,2] and John T. Harty[1,2]*

Department of Microbiology, University of Iowa, Iowa City, Iowa 52242[1]; Interdisciplinary Graduate Program in Immunology, University of Iowa, Iowa City, Iowa 52242[2]; and Department of Pathology, University of Iowa, Iowa City, Iowa 52242[3]

Received 17 February 2009/Accepted 17 June 2009

Intranasal mouse hepatitis virus type 1 (MHV-1) infection of mice induces lung pathology similar to that observed in severe acute respiratory syndrome (SARS) patients. However, the severity of MHV-1-induced pulmonary disease varies among mouse strains, and it has been suggested that differences in the host immune response might account for this variation. It has also been suggested that immunopathology may represent an important clinical feature of SARS. Little is known about the host immune response to MHV-1 and how it might contribute to some of the pathological changes detected in infected mice. In this study we show that an intact type I interferon system and the adaptive immune responses are required for controlling MHV-1 replication and preventing morbidity and mortality in resistant C57BL/6J mice after infection. The NK cell response also helps minimize the severity of illness following MHV-1 infection of C57BL/6J mice. In A/J and C3H/HeJ mice, which are highly susceptible to MHV-1-induced disease, we demonstrate that both CD4 and CD8 T cells contribute to morbidity during primary infection, and memory responses can enhance morbidity and mortality during subsequent reexposure to MHV-1. However, morbidity in A/J and C3H/HeJ mice can be minimized by treating them with immune serum prior to MHV-1 infection. Overall, our findings highlight the role of the host immune response in contributing to the pathogenesis of coronavirus-induced respiratory disease.

Severe acute respiratory syndrome (SARS) is caused by a zoonotic coronaviral infection that reached epidemic proportions beginning in late 2002 (37, 52, 55, 76, 84, 86). The etiologic agent, SARS-coronavirus (CoV), is a novel group 2 CoV that emerged in the human population exposed to infected animals that were present in wet markets in various provinces of southern China (16, 22, 35, 45, 57, 61). Although the outbreak was quickly contained by the application of aggressive public health measures, it highlighted the deadly potential of this novel pathogen as more than 8,000 people in more than 25 countries were affected, and almost 800 infected individuals died (37, 76, 84, 86). Although there have not been additional outbreaks of this disease in the general population since 2003, due to the continued presence of related viruses in bats and other animals and to cultural practices prevalent in the local population in southern China, the reemergence of this pathogen in the human population may occur in the future (40).

Currently, there are no rigorously tested efficacious prophylactic or therapeutic agents targeting this pathogen. Given the lethal potential of this virus, it is imperative to develop specific antiviral therapies that can be rapidly and universally applied. One of the serious drawbacks in the field is the paucity of appropriate animal models that faithfully reproduce the clinical features of SARS (52, 60). Although a mouse-adapted strain of this virus is available, studies with this strain need to be performed in biosafety level 3 facilities (48, 59). Logistical issues associated with such requirements hamper the rapidity and ease with which one can perform a comprehensive and detailed systemic examination of the dynamics of host-pathogen interactions. Recently, it was reported that intranasal infection of certain strains of mice with a related group 2 respiratory CoV, mouse hepatitis virus type 1 (MHV-1), induced pulmonary disease that was very similar to that observed in human subjects infected with SARS-CoV (11). In addition to the phylogenetic proximity of MHV-1 and SARS-CoV, they also share similarities in genome organization and in mechanisms of replication (63, 68). Hence, it is likely that the pathophysiology observed in MHV-1-infected mice mimics important pathological features associated with SARS-CoV infection in humans. A dysregulated immune response characterized by aberrant cytokine production is postulated to contribute to clinical disease in patients with SARS (8, 26, 55, 58, 72, 75, 82, 83). MHV-1 infection of susceptible strains of mice is also associated with an altered cytokine profile, and published reports suggest that the host immune response to the virus is an important contributor to the pathology observed in susceptible strains of mice (11). Examination of the immune response to a pathogen is critical for the purpose of designing rational and effective vaccination approaches. In addition, it also helps

* Corresponding author. Mailing address: Department of Microbiology, University of Iowa, 51 Newton Road, 3-530 Bowen Science Building, Iowa City, IA 52242. Phone: (319) 335-9720. Fax: (319) 335-9006. E-mail: john-harty@uiowa.edu.

† A.K. and S.M.H. contributed equally to this work.

‡ Present address: 354/308 IACC, Department of Chemistry, Biochemistry and Molecular Biology, North Dakota State University, Fargo, ND 58105.

▽ Published ahead of print on 1 July 2009.

identify potentially deleterious effects of the immune response that can subsequently be manipulated to the advantage of the host, thereby maximizing recovery and minimizing morbidity.

In the present study we have carried out a comprehensive analysis of the immune response to MHV-1 following intranasal infection of both resistant and susceptible strains of inbred mice. Our observations in alpha/beta interferon (type I IFN) receptor-knockout (IFN-αβR-KO) mice and NK cell-depleted mice shed light on the protective role of these components of the innate immune response in resistant C57BL/6J (B6) mice. And our examination of the adaptive immune responses to MHV-1 shows that they function as a double-edged sword, mediating protection in resistant strains and contributing to pathology in susceptible strains of mice.

MATERIALS AND METHODS

Mice. Five- to seven-week-old female A/J (H-2^a), C3H/HeJ (H-2^k), BALB/c (H-2^d), and B6 (H-2^b) mice were purchased from the National Cancer Institute (NCI, Frederick, MD). B6-IFN-αβR-KO mice (47) were originally obtained from Matthew Mescher (University of Minnesota, Minneapolis, MN). B6 tumor necrosis factor alpha -deficient (B6-TNFKO) mice (51) were originally obtained on a 129/SV×B6 background from George Kollias and were backcrossed to B6 mice >12 generations to generate B6-TNFKO mice. B6-IFN-γ-deficient (B6-GKO) mice, B6-perforin-deficient (B6-PFP) mice, and B6-Rag1-knockout (B6-Rag1-KO) mice were originally purchased from the Jackson Laboratory (Bar Harbor, ME). Knockout strains of mice were maintained by brother-sister mating, and all mice were housed under specific-pathogen-free conditions at the University of Iowa (Iowa City, IA) animal care unit until the time of infection, at which point the mice were transferred to housing at the appropriate biosafety level. All animals were maintained in accredited facilities at the University of Iowa (Iowa City, IA) and used in accordance with the guidelines established by the University of Iowa animal care and use committee. Mice were infected at 8 to 9 weeks of age.

Virus. Parent stock of MHV-1 was obtained from the American Type Culture Collection (ATCC, Manassas, VA). To propagate this virus, DBT cells were infected with this parent stock at a multiplicity of infection of 0.1. Briefly, DBT cells were grown to about 80 to 90% confluence in T25 flasks in Dulbecco's modified Eagle's medium (DMEM; Gibco, Grand Island, NY) supplemented with 10% fetal calf serum (FCS; Atlanta Biologicals, Norcross, GA), 10 U/ml penicillin G (Gibco, Grand Island, NY), and 10 μg/ml streptomycin sulfate (Gibco) (referred to herein as complete DMEM). At the time of infection, the medium in the flask was removed, and the appropriate amount of virus was diluted in 1 ml of serum-free DMEM and added to the monolayer. The virus was allowed to adsorb onto the cells for 30 min with gentle rocking every 10 to 15 min. After 30 min, 11 ml of complete DMEM was added to the flask, and cells were incubated at 37°C for 24 h. The culture was subsequently subjected to multiple freeze-thaw cycles; the cell suspension was harvested and spun, the supernatant containing the virus particles was aliquoted, and virus titers were determined.

Virus titers. Titers of replicating virus were determined by a standard plaque assay. HeLa cells (ATCC) stably transfected with the MHV receptor (18) were grown to 90% confluence in six-well plates using complete DMEM. Serial 10-fold dilutions of either virus stock or organ homogenates from infected mice were prepared in serum-free DMEM and added onto the monolayers (100 μl/well) and allowed to adsorb for 30 min, following which 2 ml of complete DMEM was added to each well. After 24 h a 1:1 overlay mixture consisting of 2× minimal essential medium (Invitrogen, Carlsbad, CA) supplemented with 4% FCS (Atlanta Biologicals), 10 U/ml penicillin G, 10 μg/ml streptomycin sulfate, 0.26% sodium bicarbonate solution (Gibco), and 1.8% SeaKem ME agarose (Cambrex, North Brunswick, NJ) was prepared. To this mixture was added 0.01% neutral red (Sigma, St. Louis, MO). The supernatant from each well was aspirated and replaced with the overlay mixture and incubated at 37°C for 2 to 4 h, following which plaques were counted with the assistance of a light box. Mean neutralization antibody titers were determined by a constant virus-variable serum plaque reduction assay performed as previously described (56).

Virus infection of mice. For intranasal infections, mice were anesthetized with avertin (2,2,2-tribromoethanol; Aldrich, Milwaukee, WI) intraperitoneally (i.p.) and administered a sublethal dose of MHV-1 intranasally in a volume of 50 μl. The sublethal dose was determined to vary among strains, and this dosage was recalibrated for subsequent experiments and was based on the estimation of the lethal dose as follows: for B6 and BALB/c mice, $>10^5$ PFU; for A/J mice, $>10^4$ PFU; and for C3H/HeJ mice, $>(5 \times 10^3)$ PFU. Evaluation of disease in B6-PFP, B6-GKO, and B6-TNFKO mice was done after intranasal infection with 10^5 PFU of MHV-1 in a volume of 20 μl. For adoptive transfer studies, memory splenocytes were obtained from donor mice that had been previously infected with 2×10^5 PFU of MHV-1 i.p. For the evaluation of weight loss after infection, the weight of each mouse was normalized to 100% at the time of infection (day 0), and subsequent weight measurements were recorded at defined time points after infection. Weight data are presented as the mean percentage of the starting weight ± standard error of the mean (SEM).

Antibody treatments. Depletion of specific subsets of immune cells was induced by antibody treatment of mice. NK cells were depleted in B6 mice using a purified monoclonal antibody targeting NK1.1 (clone PK136; a gift from Jonathan Heusel, University of Iowa, Iowa City, IA). Mice were injected with 200 μg administered i.p. 48 and 24 h prior to infection. Control mice in the same experiment were treated with purified mouse monoclonal antibody SF1-1.1.10 (anti-H-$2K^d$; ATCC, Manassas, VA). Depletion of CD4 and CD8 T cells was induced by treating mice i.p. with 400 μg/mouse of purified rat anti-mouse CD4 (clone GK1.5; ATCC, Manassas, VA) and CD8 (2.43; ATCC, Manassas, VA), respectively, on days −1, +1, and +7 with respect to infection. Control mice received identical amounts of purified rat immunoglobulin G (IgG) (MP Biomedicals, Solon, OH).

Passive immunization. Serum was obtained by serially bleeding A/J and C3H/HeJ mice that had been intranasally infected with MHV-1 3 to 6 months previously. Naïve recipients were administered 300 μl/mouse of undiluted pooled serum from syngeneic donors 1 day prior to infection. Control recipients received identical amounts of undiluted pooled serum from naïve syngeneic donors prior to infection.

Adoptive transfer. Naïve recipients received 2×10^7 bulk splenocytes from either naïve or previously immunized syngeneic donors. In some experiments recipient mice were treated with physiologically relevant numbers of CD4 (4.3×10^6 cells/mouse) or CD8 (1.8×10^6 cells/mouse) T cells purified from the spleens of previously immunized donor mice using negative selection on an Automacs machine (Miltenyi-Biotec, Germany).

Lung function. Development of baseline airway resistance as determined by the measurement of the parameter enhanced pause (Penh) was evaluated using a whole-body plethysmograph from Buxco Electronics, Inc (Troy, NY).

Lung histology. Whole lungs with the heart attached were harvested from C3H/HeJ mice treated with rat IgG or anti-CD4 and anti-CD8 antibodies at day 10 after intranasal MHV-1 infection. Lungs were fixed in 10% neutral buffered formalin (Fisher Scientific, Pittsburgh, PA) prior to being processed and paraffin embedded at the University of Iowa Comparative Pathology Laboratory. Paraffin blocks were sectioned at a 5-mm thickness. Sections were stained with hematoxylin and eosin at the University of Iowa Central Microscopy Core.

Histopathologic examination and scoring. The tissue sections were examined by a board-certified veterinary pathologist who was blinded to the study groups. Tissues were initially screened to define the breadth of morphological parameters that were of interest for subsequent histopathologic grading. Lesions in connecting airways, alveoli, and interstitia; vascular leukocyte margination; and development of alveolar fibrin and edema were evaluated and graded for distribution and severity in tissue sections. The distribution of lesions in alveoli, interstitia, and vessels was graded as follows: 1, normal to rare change; 2, less than one-third affected; 3, more than one-third but less than two-thirds affected; 4, more than two-thirds affected. Edema was defined as eosinophilic seroproteinaceous fluid within the alveolar lumen. A similar grading scale was used to describe the extent of tissue fields affected by alveolar fibrin deposition and edema formation.

Enzyme-linked immunosorbent assay (ELISA). Nunc-Immuno plates (Nalge Nunc International) were coated overnight at 4°C with 2 μg/ml of capture antibody (R&D Systems) in 0.1 M Na_2HPO_4 (pH 9.0). After plates were washed with phosphate-buffered saline–0.5% Tween 20 (Sigma Aldrich), they were blocked with RPMI 1640 medium supplemented as described for at least 2 h at room temperature. Whole lungs were harvested and homogenized using glass douncers (Kontes Glass) in 1 ml of RPMI 1640 medium supplemented as described and containing a 1/200 dilution of protease inhibitor mix (Sigma Aldrich). Lung homogenates were centrifuged, and 50 μl of supernatant was added to the wells and incubated overnight at 4°C. Recombinant murine IFN-γ, TNF-α, MCP-1 (monocyte chemotactic protein 1), and interleukin-10 (IL-10) (R&D Systems) were diluted in phosphate-buffered saline plus 10% FCS and used to calculate standard curves. Cytokine was detected by incubation with 0.1 μg/ml biotinylated anti-chemokine/cytokine antibody (R&D Systems) for 2 h at room temperature. Avidin-peroxidase (1:400 dilution; Sigma-Aldrich) was added for

30 min before plates were developed with 3,3′,5,5′-tetramethylbenzidine dihydrochloride (Sigma-Aldrich). The reaction was stopped after 5 min with 2N H_2SO_4 (Ricca Chemical). Plates were read at 450 nm using an ELx800 plate reader and analyzed using KC Junior software (both from Bio-Tek Instruments).

Immunophenotyping. Lungs were harvested following perfusion from C3H/HeJ mice treated with rat IgG or anti-CD4 and anti-CD8 antibodies at day 10 after intranasal MHV-1 infection. Single-cell suspensions of lungs of individual mice were prepared by mashing through metal screens. Red blood cells were removed using ammonium chloride-kalium lysis buffer, and cells were resuspended on ice in RPMI 1640 medium containing 10% FCS, penicillin-streptomycin, L-glutamine, and 2-mercaptoethanol. Cells were stained with the following fluorochrome-conjugated rat anti-mouse monoclonal antibodies: CD4-fluorescein isothiocyanate (FITC; clone RM4-4), CD8β-phycoerythrin (PE), CD3ε-allophycocyanin, CD19-FITC, B220-peridinin chlorophyll protein-Cy5.5, DX5-PE, Ly6C-FITC, Ly6G-PE, CD11c-allophycocyanin, major histocompatibility complex class II-peridinin chlorophyll protein-Cy5.5, CD11b-PE-Cy7 (all from eBioscience, San Diego, CA), and Siglec-F-PE (BD Pharmingen, San Diego, CA). Samples were acquired on a FACSCanto flow cytometer (Becton Dickinson, San Jose, CA) and analyzed using FlowJo software (Tree Star, Inc, Oregon).

Statistical analysis. All statistical analyses were performed using GraphPad software (San Diego, CA). Statistical significance was determined using an unpaired Student's *t* test. A P value of <0.05 was considered statistically significant.

RESULTS

C3H/HeJ mice are most susceptible to intranasal MHV-1 infection-induced disease. It has been previously established that intranasal MHV-1 infection of certain inbred strains of mice serves as a clinically relevant small-animal model to study SARS (11). MHV-1-induced pulmonary disease of varying severity occurred in BALB/cJ, B6, C3H/St, and A/J mice (11). Of these strains, A/J mice were found to be the most susceptible, whereas the B6 mice appeared to be the most resistant (11).

Consistent with the results of De Albuquerque et al. (11), our initial study (30) also demonstrated a similar susceptibility in A/J mice, partial resistance in BALB/cJ mice, and complete resistance in B6 mice following intranasal MHV-1 infection (5×10^3 PFU/mouse). Additionally, our analysis revealed that C3H/HeJ mice are also very susceptible to MHV-1-induced disease.

Based on these observations, we initiated a virus-dose titration analysis to identify viral input doses that would induce overt signs of disease and mortality in both resistant and susceptible strains of mice. This analysis indicated that morbidity and mortality following infection varied considerably among the strains, depending on the input dose of the virus. B6 mice easily tolerated doses in excess of 10^5 PFU/mouse, displaying only mild weight loss (~10% of starting weight) early after infection, followed by recovery by day 7 to 8 postinfection (data not shown). In contrast, significant mortality was observed in C3H/HeJ mice with a dose of 10^4 PFU/mouse (data not shown). For all studies done subsequently, mice were inoculated with the appropriate dose that established a predominantly sublethal infection that ensured that the majority of the mice survived the pathogenic insult (see "Virus infection of mice" above for lethal doses).

We previously showed that the strain-specific differences in susceptibility to disease were not due to differences in the kinetics of virus clearance or tissue tropism (30). However, we did observe an early onset of morbidity in C3H/HeJ, A/J, and even BALB/c mice at days 2 to 4 postinfection, with a subsequent peak in the severity of symptoms between days 7 to 10 postinfection (30). In addition, we observed occasional mortality following sublethal infection within this latter window. These findings support earlier observations suggesting a potential link between the immune response and disease development in MHV-1-infected mice (11), and they further indicated a potential role for both the early innate immune responses as well as the later adaptive immune responses in the pathogenesis of MHV-1-induced disease.

Type I IFN-mediated signaling is an important contributor to the innate resistance of B6 mice to intranasal MHV-1 infection-induced disease. Several reports suggest that type I IFNs play a critical role in the context of CoV infections (9, 13, 87). In one study SARS patients treated with IFN-α experienced faster improvement in clinical signs and symptoms than patients maintained on corticosteroid therapy alone (42). Another study reported that the infected lungs from resistant B6 mice displayed increased expression of type I IFN genes compared to the lungs of the susceptible A/J mice following intranasal MHV-1 infection (11). To directly examine the role of type I IFNs in the context of intranasal MHV-1 infection, we compared weight loss and survival between resistant wild-type B6 mice and B6 mice genetically deficient in the receptor for IFN-αβ. These knockout mice are capable of producing type I IFNs, but the absence of the relevant receptor abolishes type I IFN-mediated signaling (47). We observed that the absence of type I IFN-mediated signaling severely compromised the innate resistance of the B6 mice as the type I IFN-αβR-KO mice progressively lost weight, and all mice died by day 5 postinfection (Fig. 1). Furthermore, analysis of tissues harvested from mice at day 3 postinfection revealed that the titers of replicating virus were higher in the IFN-αβR-KO mice than in the wild-type controls (Fig. 2A to D).

Infection of mice with the JHM strain of MHV is associated with an early recruitment of functional NK cells although they are not considered to be essential for mediating viral clearance and affecting the outcome of infection in mice with an intact immune system (66, 67, 74). A recent report showed that one of the important functions of type I IFNs may include the optimal priming and effector activity of NK cells (44). Based on this information and our data from infected IFN-αβR-KO mice, we next investigated whether depleting NK cells in B6 mice would impact the course of MHV-1-induced disease. B6 mice were treated with either a control antibody or the NK cell-depleting antibody PK136 at 48 and 24 h prior to infection. This monoclonal antibody targets the NK1.1 molecule, a pan-NK cell marker expressed in B6 mice. Analysis of the spleens of antibody-treated naïve mice on the day of infection (day 0) indicated that PK136 treatment resulted in an 80% reduction in the fraction of detectable $CD3^-$ $DX5^+$ $CD122^+$ cells (data not shown). All NK cell-depleted B6 mice lost more body weight after MHV-1 infection, and this weight loss was significantly greater than that in control antibody-treated mice at days 7 and 10 postinfection. However, the majority of NK cell-depleted B6 mice survived the infection and showed signs of recovery (Fig. 1). This enhanced morbidity of the NK cell-depleted mice was not the result of a compromised ability to control virus as plaque assay data showed that virus titers were similar to those of the control antibody-treated mice (Fig. 2). These results are similar to previously published reports showing that NK cells do not play an important role in the clearance of the JHM strain of MHV (66, 67, 74). In contrast, the ability

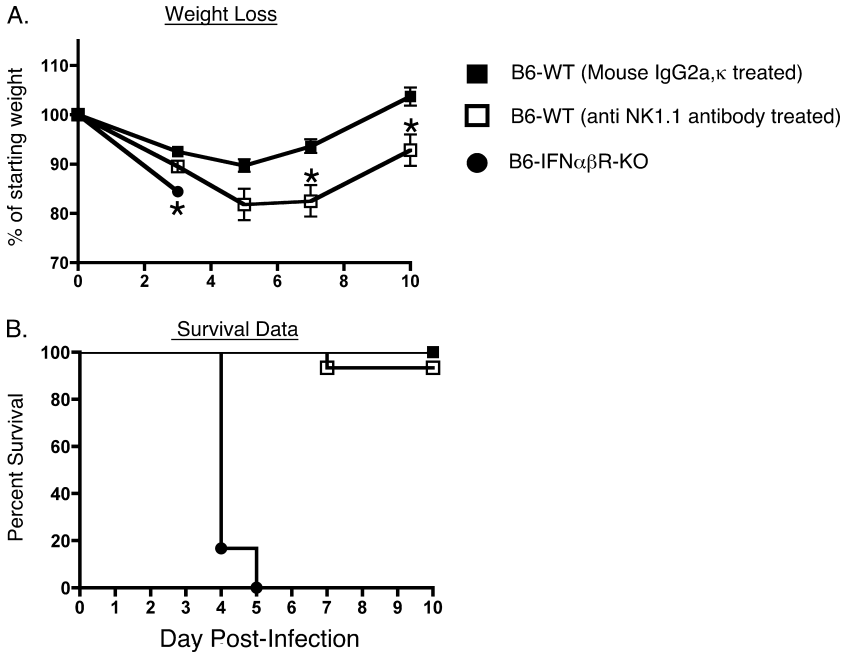

FIG. 1. Protective role of type I IFN during intranasal MHV-1 infection of B6 mice. B6 wild-type (WT) mice were treated with either 200 μg of purified mouse IgG2a or anti-mouse NK1.1 (clone PK136) monoclonal antibody at 48 and 24 h prior to intranasal MHV-1 infection (10^5 PFU/mouse). Untreated B6-IFN-αβR-KO mice were also included in this analysis. A total of 5 to 10 mice were evaluated in each group for weight loss and survival for 10 days following infection. (A) Changes in body weight after infection were measured at the indicated time points. Statistically significant differences between the mean weights of B6 mice treated with mouse IgG2a and the other two groups of mice at each time point were determined using an unpaired Student's *t* test and are indicated by an asterisk. (B) Kaplan-Meier survival curves depict the percentage of surviving mice in each group at the indicated time points following infection.

of NK cells to reduce morbidity in resistant B6 mice after MHV-1 infection is opposite to their minimal contribution to resistance following infection with the JHM strain of MHV. Collectively, our data show that both type I IFN-mediated signaling and NK cells contribute to reducing morbidity and mortality in MHV-1-infected B6 mice.

Susceptibility to MHV-1-induced disease is enhanced in B6-Rag1-KO mice. In addition to the innate immune response, the adaptive immune response is also critical for the rapid resolution of infections (2, 20, 31, 64, 89). This phase of the host response is detectable a few days after the initiation of the innate response, and it is comprised of B and T cells that identify pathogen-specific determinants expressed by cell-free and cell-associated forms of the pathogen (2, 7, 20, 31, 64, 89). Our previous data showed that B6 mice reveal no overt signs of disease following intranasal infection with 5×10^3 PFU/mouse of MHV-1 (30). This resistant phenotype is largely preserved even at doses as high as 10^5 PFU/mouse, but at this higher dose the mice did experience ~10% loss in body weight up until days 5 to 6 postinfection, after which they rapidly regained weight to preinfection levels (Fig. 3A). In order to examine the contribution of the adaptive immune response in preserving the resistant phenotype of the B6 mice, we analyzed both wild-type B6 mice and B6-Rag1-KO mice, which lack both T and B cells (46), following intranasal MHV-1 infection (10^5 PFU/mouse). Similar to the control wild-type mice, the B6-Rag1-KO mice experienced about a 10% loss in body weight up to day 7 postinfection. Beyond this time point the wild-type mice rapidly recovered as expected; however, the Rag1-KO mice continued on a downhill course, progressively losing more weight and exhibiting increased mortality starting around day 13 postinfection (Fig. 3A and B). Quantifying the virus titers in these mice showed that, whereas the titers were similar to those of wild-type controls measured at day 3 postinfection, the lack of an appropriate adaptive immune response markedly impaired the ability of the B6-Rag1-KO mice to control virus replication in tissues at a later time point (day 10 postinfection) (Fig. 2). Overall, these data demonstrate not only that the resistance of B6 mice to MHV-1-induced disease is influenced by the innate immune response to the virus but also that MHV-1-specific T- and B-cell responses exert a crucial protective function that helps minimize morbidity.

It has been shown that perforin and IFN-γ are required for CD8 T-cell-mediated control of JHM-MHV-mediated central nervous system (CNS) infections and associated morbidity (3, 41, 50). These molecules are expressed by both innate and adaptive components of the host immune system and collectively are vital to their ability to eliminate a number of pathogenic invaders (19, 20). We also evaluated the outcome of intranasal MHV-1 infection in B6 mice that lacked either IFN-γ, TNF-α, or perforin. Interestingly, we observed that the absence of any of these molecules individually did not compromise the resistance of B6 mice to MHV-1 infection (Fig. 3C). These results suggest the presence of a redundancy in the host immune system whereby one effector molecule can effectively compensate for the selective absence of another to combat MHV-1-induced disease.

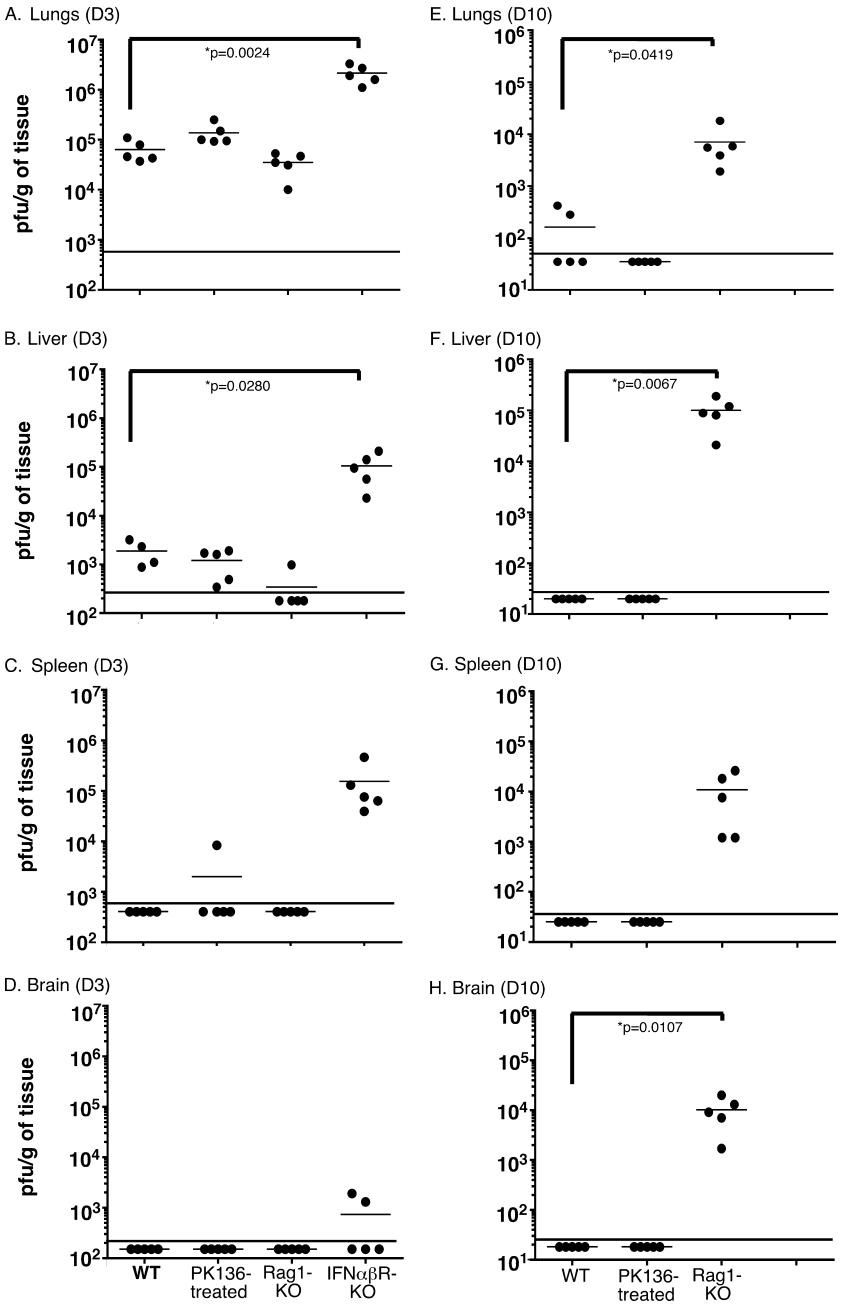

FIG. 2. MHV-1 replication is controlled by both innate and adaptive immune responses. Virus titers were measured by plaque assays in the lungs, livers, spleens, and brains of wild-type (WT) B6 mice, anti-NK1.1-treated B6 mice, B6-Rag1-KO mice, and B6-IFN-αβR-KO mice 3 days (D3) and 10 days (D10) after intranasal infection with MHV-1 (10^5 PFU/mouse). All B6-IFN-αβR-KO mice succumbed to infection prior to day 10. Five mice per group were analyzed at each time point, and data are represented as the number of PFU/g of tissue from individual mice. Statistically significant differences in titers between wild-type B6 mice and the rest of the experimental groups were determined using an unpaired Student's *t* test and are indicated by an asterisk. The limit of detection is indicated in each graph by the horizontal line parallel to the *x* axis; mouse groups are indicated on the *x* axes of panels D and H, and values in graphs above are aligned similarly.

Adoptive transfer of immune serum into naïve hosts significantly reduces morbidity and systemic viral burden in mice susceptible to MHV-1-induced disease. Based on our data obtained from B6-Rag1-KO mice, we wanted to further dissect the role of the adaptive immune system in the context of MHV-1 infection. We decided to focus this investigation using susceptible strains of mice as this would allow us to more decisively discern the exact role of T and B cells in mediating the development of disease. In order to define the contribution of the MHV-1-specific antibody response during the course of infection, naïve C3H/HeJ and A/J recipients were treated with either immune serum or serum obtained from syngeneic naïve hosts 24 h prior to infection. Immune serum was obtained from syngeneic mice that had been infected intranasally 3 to 6

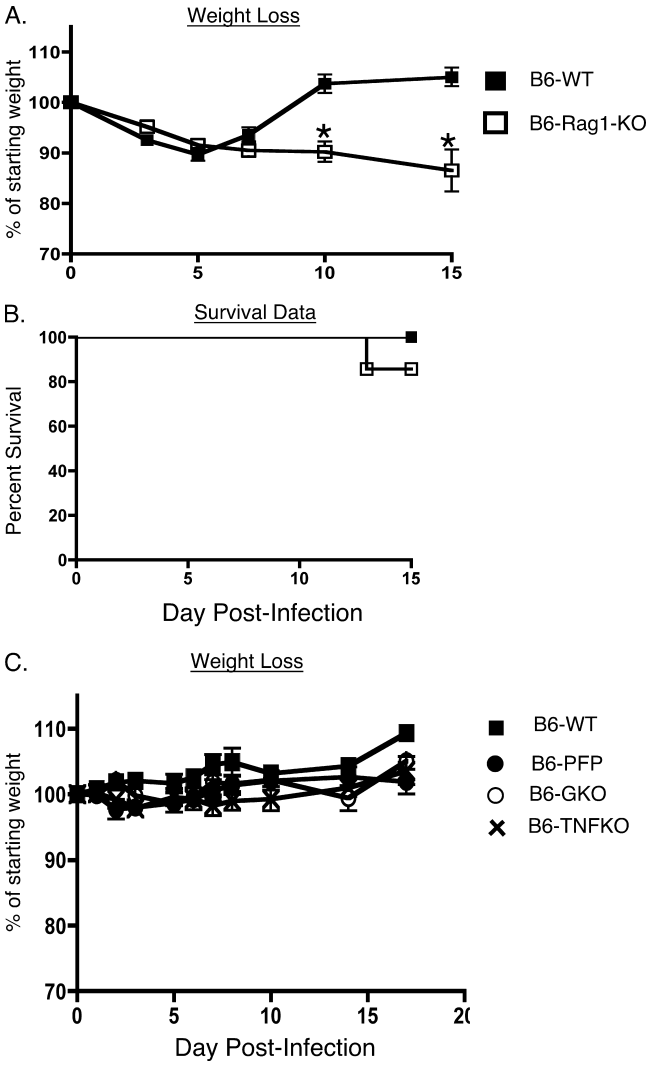

FIG. 3. Susceptibility to MHV-1 infection is enhanced in Rag1-KO mice. B6 wild-type (WT), B6-PFP, B6-GKO, B6-TNFKO, and B6-Rag1-KO mice were intranasally infected with 10^5 PFU/mouse of MHV-1. A total of 5 to 10 mice were evaluated in each group, and mice were followed for weight loss (A and C) and survival (B) for 15 days following infection. Statistically significant differences in the mean weights of mice between the two groups were determined using an unpaired Student's *t* test and are indicated by an asterisk. Survival data are represented by Kaplan-Meier curves indicating the percentage of mice that survived the infection.

months previously with MHV-1. Mice were followed for weight loss, and 4 days after infection the recipient mice were sacrificed to determine systemic viral burden. We observed that the mice that were treated with naïve serum progressively lost a significant amount of weight following infection, whereas the mice that received immune serum did not exhibit weight loss (Fig. 4A). Additionally, the virus titers were significantly reduced in the lungs, livers, and spleens of A/J mice treated with immune serum compared to mice that did not receive immune serum. Similarly, virus titers were significantly reduced in the lungs and spleens of C3H/HeJ recipients of immune serum, and the titers were also markedly reduced in the livers of these mice in comparison to controls. However, owing to the greater variation in the levels of replicating virus measured in the livers of passively immunized C3H/HeJ mice, this reduction did not achieve statistical significance (Fig. 4B to D). In order to establish that this protective effect in immune-serum-recipient mice was mediated by MHV-1-specific neutralizing antibodies, we calculated the mean neutralizing antibody titer in the pooled sera of previously immunized donor mice by performing a constant virus-variable serum plaque reduction assay (56). The neutralization titer is the reciprocal of the dilution of immune serum yielding a 50% reduction in the number of MHV-1 PFU on HeLa-MHV-R cells. This titer was 1:4,943 in C3H/HeJ mice and greater than 1:10,000 in A/J mice. These data reveal that intranasal MHV-1 infection generates a robust neutralizing antibody response that is very effective at combating subsequent MHV-1 infections, reducing viral burden, and alleviating morbidity.

T-cell responses contribute to the development of disease in MHV-1-infected C3H/HeJ and A/J mice. It has been previously documented that the transfer of T cells into MHV-infected Rag1-KO mice induces demyelination in the CNS (23, 77). However, T-cell-mediated immunopathology has not been described in immunocompetent mice infected with CoVs. In order to examine the role of T cells following intranasal MHV-1 infection of mice that possess an intact T-cell compartment, we treated naïve C3H/HeJ and A/J recipients with 400 μg of depleting anti-mouse CD4 and CD8 antibodies delivered i.p. on days −1 and 0 and then again on day 7 postinfection. The efficacy of depletion was previously tested in a separate group of naïve mice where antibody treatment on two consecutive days resulted in a 93% reduction in the fraction of CD4 T cells and 99% reduction in CD8 T cells measured in peripheral blood mononuclear cells 2 days after the last treatment. Analysis of peripheral blood mononuclear cells of these mice 17 days after the last treatment revealed that depletion was maintained at 88% for the CD4 T cells and at 98% for the CD8 T cells (data not shown). Control mice received identical amounts of purified rat IgG at the same time points. The mice were followed for weight loss and illness and were also monitored for changes in Penh at selected time points after infection. Both the control group and T-cell-depleting antibody-treated groups exhibited morbidity and progressively lost weight following infection. The control group of mice continued to steadily lose weight up until day 10 postinfection, after which they began to gradually recover. In contrast, the mice that had been treated with the T-cell-depleting antibody recovered faster and began regaining the lost weight around day 7 postinfection (Fig. 5A and C). Depleting T cells had a beneficial effect on lung function, as evidenced by a more rapid reduction in Penh values in these mice compared with the control group of mice (Fig. 5B and D).

We also evaluated mice that were treated with either the CD4- or CD8-depleting antibody. Depletion of just one subset in both A/J and C3H/HeJ mice yielded an illness/recovery pattern that was intermediate between the control group and the group that received both depleting antibodies simultaneously (Fig. 5). These data suggest that both CD4 and CD8 T cells might be contributing to the development of lung pathology following intranasal MHV-1 infection.

Unexpectedly, we did observe some mortality in both A/J and C3H/HeJ mice during the course of this experiment. Three

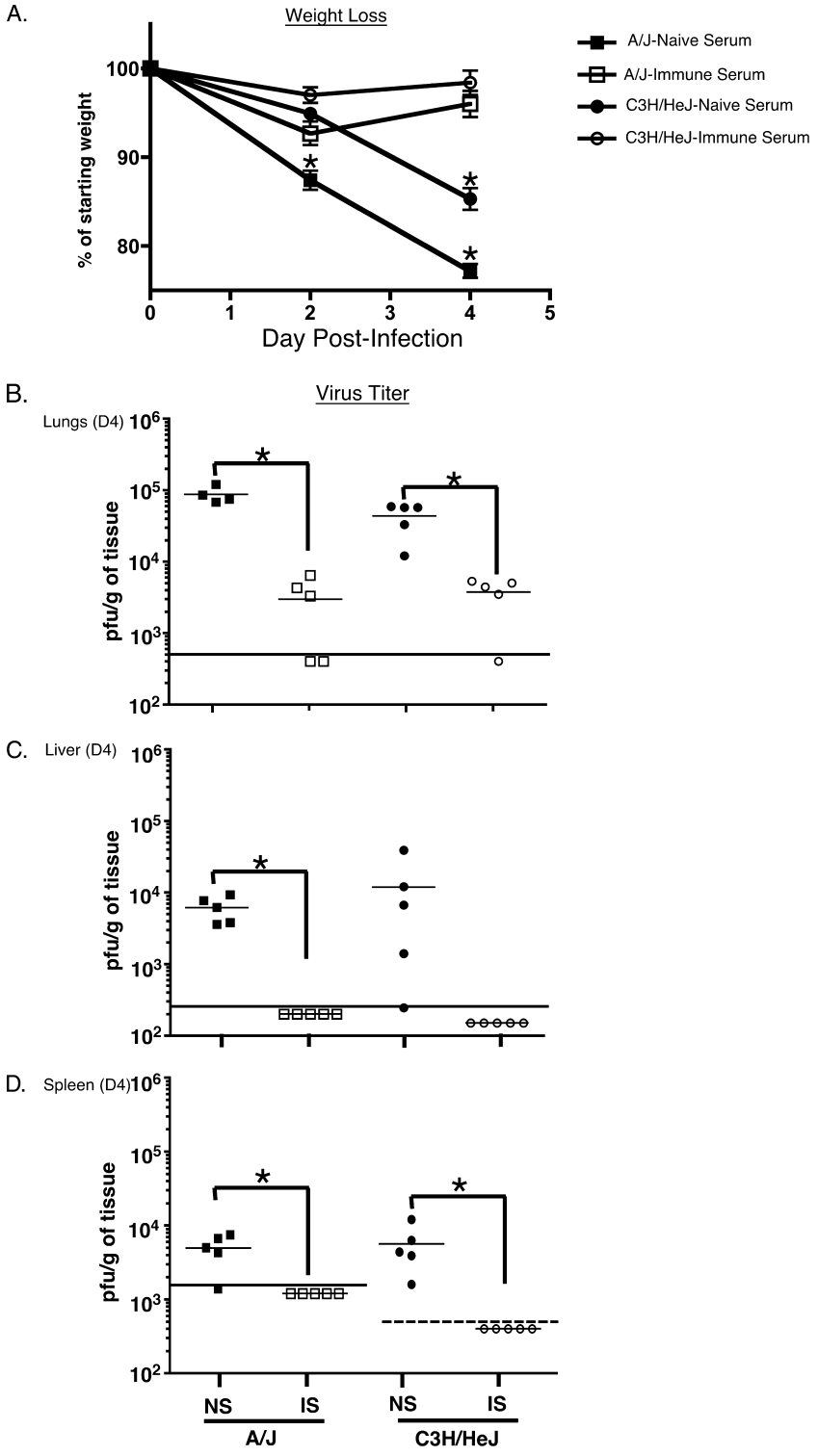

FIG. 4. Passive immunization can control infection and morbidity following intranasal MHV-1 infection in susceptible strains of mice. A/J and C3H/HeJ mice (5 mice/group) received 300 μl of serum pooled from either naïve syngeneic donors or from syngeneic donor mice that had been infected intranasally 3 to 6 months previously with MHV-1. One day later all mice were intranasally infected with 1.5×10^4 PFU/mouse of MHV-1. (A) Weight loss in recipient mice was measured at the time points indicated. Statistically significant differences between the weights of mice treated with naïve serum and those treated with immune serum were determined using an unpaired Student's *t* test and are indicated by an asterisk. (B to D) Mice were euthanized on day 4 (D4) after infection, and virus titers were determined by plaque assays in lungs, livers, and spleens and are represented as the number of PFU/g. Statistically significant differences between virus titers in mice treated with naïve serum (NS) and those treated with immune serum (IS) were determined using an unpaired Student's *t* test and are indicated by an asterisk. The limit of detection is indicated in each graph by the horizontal line parallel to the *x* axis. The limit of detection in the spleens of C3H/HeJ mice is lower than that in the spleens A/J mice and is indicated by the dashed line.

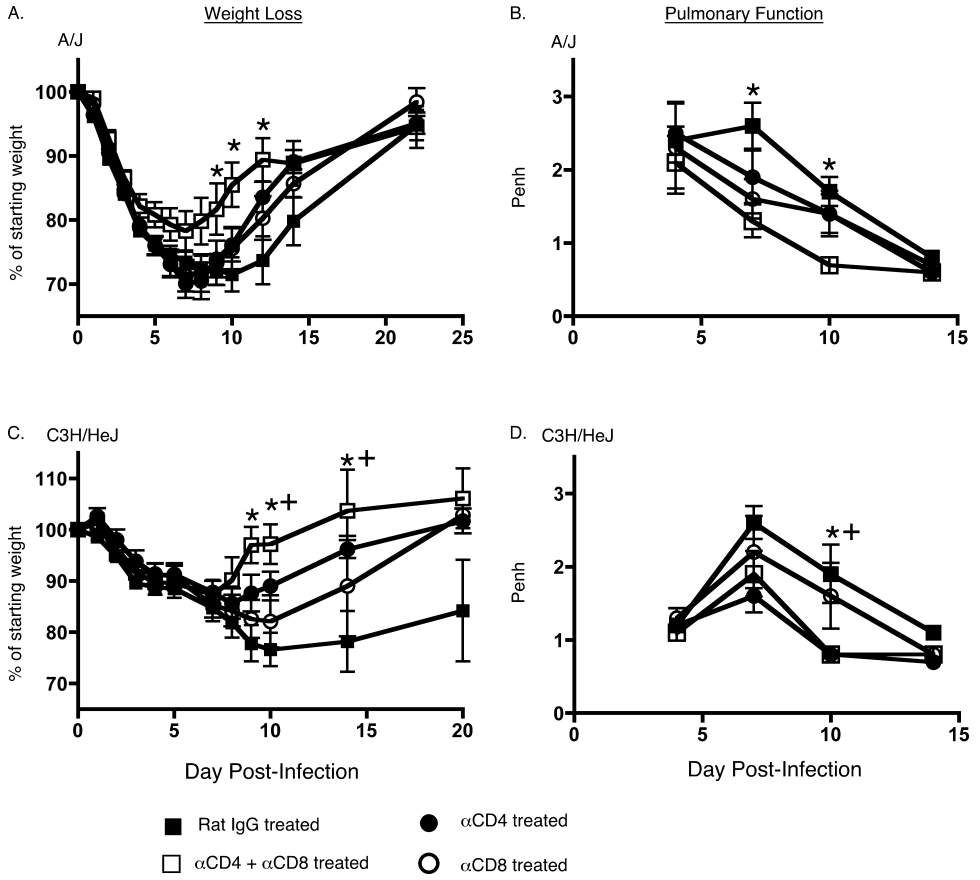

FIG. 5. Reduced morbidity of MHV-1-infected A/J and C3H/HeJ mice following depletion of CD4 and CD8 T cells. A/J or C3H/HeJ mice (5 mice/group) were treated with 400 μg of either purified rat IgG or rat anti-mouse CD4 (clone GK1.5) or rat anti-mouse CD8 (clone 2.43) or both rat anti-mouse CD4 and CD8 1 day prior to, on the day of, and 7 days after intranasal infection with 5×10^3 PFU/mouse of MHV-1. (A and C) Changes in body weight were monitored at the indicated time points. Statistically significant differences in the mean weights of mice treated with the control antibody and mice treated with both anti-CD4 and anti-CD8 antibodies were determined using an unpaired Student's *t* test and are indicated by an asterisk (*). Statistically significant differences between the mean weights of mice treated with the control antibody and the group of mice treated with the anti-CD4 antibody are indicated by a plus (+) symbol. No statistically significant differences were observed between the mean weights of mice treated with the control antibody and the groups of mice treated with the anti-CD8 antibody. These weight loss data are representative of two independent experiments. (B and D) Penh was determined using a whole-body plethysmograph at the indicated time points. Data are shown as means ± SEM, and statistically significant differences between the Penh values of control mice and mice depleted of both CD4 CD8 T cells were determined using an unpaired Student's *t* test and are indicated by an asterisk (*). Statistically significant differences between the Penh values of mice treated with the control antibody and the groups of mice treated with the anti-CD4 antibody are indicated by a plus (+) symbol. No statistically significant differences were observed between the Penh values of mice treated with the control antibody and the groups of mice treated with the anti-CD8 antibody. α, anti.

out of 15 A/J mice that received the control antibody and 1 out of 10 A/J mice that received the T-cell-depleting antibody died. One C3H/HeJ mouse from the control group and two that received the T-cell depletion treatment also did not survive. All of the deaths in the T-cell-depleting antibody-treated mice occurred between days 8 and 10 postinfection. Whereas a small degree of mortality is observed following sublethal infection, the occurrence of mortality in the T-cell-depleted mice was unexpected, given their overall faster improvement in disease status. Experiments are currently under way to investigate the potential cause(s) of death in the T-cell-depleted mice.

These results demonstrate that, in contrast to the protective role of the adaptive immune response in resistant B6 mice after MHV-1 infection, in A/J and C3H/HeJ mice, which are susceptible to MHV-1 induced disease, T cells contribute significantly to the development of disease. Overall, these results are suggestive of an inherent duality in the nature of the host immune responses. Whereas the T-cell responses can contribute to the reduction in systemic viral burden, the elaboration of their effector functions including potentially massive cytokine release can also induce immunopathology that contributes to morbidity and mortality in the affected host (1, 36).

T-cell-depleting monoclonal antibody treatment of mice reduces pathology in the lungs of MHV-1-susceptible mice. Our evaluation of MHV-1-susceptible C3H/HeJ and A/J mice revealed that depletion of CD4 and CD8 T cells at the time of primary infection minimized morbidity, as determined by measuring weight loss and the development of airway resistance, suggesting that T cells were contributing to the pathology in these mice following infection (Fig. 5). To determine how T cells exacerbated pathology, we harvested lungs for tissue histology, cytokine/chemokine production, and immunopheno-

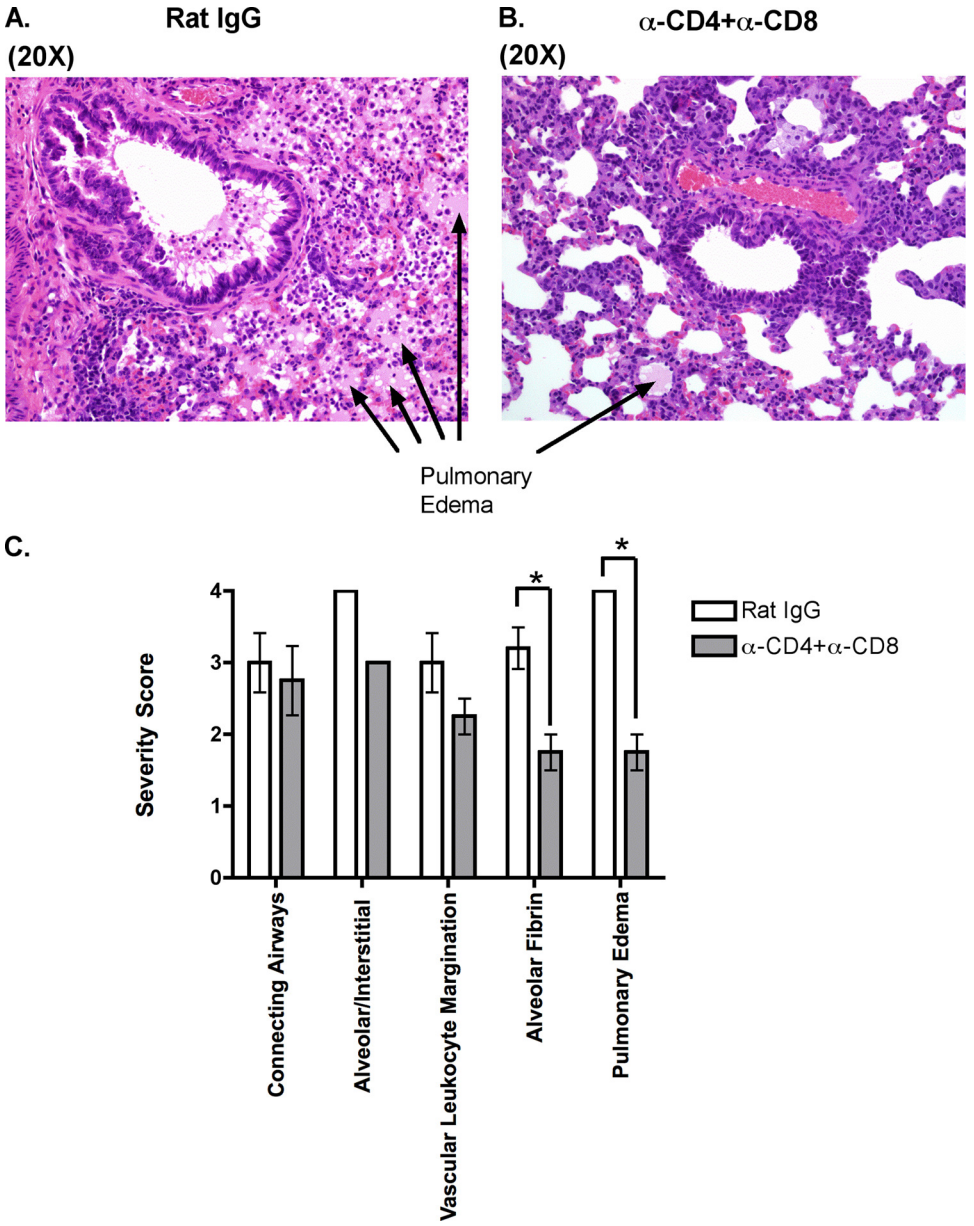

FIG. 6. T-cell-dependent development of pulmonary pathology in MHV-1-infected mice. Whole lungs were harvested at day 10 postinfection with MHV-1 from C3H/HeJ mice treated with either rat IgG or anti-CD4 plus anti-CD8 monoclonal antibody as described in Materials and Methods. Hematoxylin and eosin sections were prepared as described in Materials and Methods (A and B). Slides were evaluated for fibrin deposition in alveoli and the development of pulmonary edema according to the severity grading scale described in the Materials and Methods (C). Data are shown as means ± SEM, and statistically significant differences between control mice and mice treated with both anti-CD4 and anti-CD8 monoclonal antibodies were determined using an unpaired Student's *t* test and are indicated by an asterisk. α, anti.

typic analysis from control or T-cell-depleted MHV-1-infected C3H/HeJ mice. The lungs were harvested on day 10 postinfection as our initial evaluation had revealed the biggest difference in morbidity between control and T-cell-depleted mice and at this time point. Tissue histology was examined by a board-certified veterinary pathologist who was blinded to the study groups. The mice that were treated with rat IgG had more severe pathology than the mice treated with anti-$CD4^+$ anti-CD8 monoclonal antibodies based on morphology, principally on the extent of edema with admixed fibrin and necrosis (Fig. 6). Airways were, in comparison to alveoli/interstitial compartments, less affected and had variable accumulation of cellular debris, leukocytes, mucus, and occasional obstruction by edema in some distal airways. We also measured the level of cytokines/chemokines in supernatants of lung homogenates obtained from similarly treated MHV-1-infected mice. Our analysis revealed that levels of IFN-γ as determined by ELISA were lower in the lungs of mice treated with both anti-CD4 and anti-CD8 monoclonal antibodies although this difference did not reach statistical significance (data not shown). We did not observe any statistically significant difference between the groups for the presence of MCP-1 and TNF-α. IL-10 levels

were below the limit of detection in both groups (data not shown). Interestingly, our phenotypic analysis of cellular subsets in the bulk lung population of control mice and those treated with T-cell-depleting antibodies demonstrated a significantly higher ($P < 0.05$) proportion and total number of alveolar macrophages ($CD11c^+$ Siglec-F positive [Siglec-F^+]) (65) in the lungs of the latter group even though bulk lung cellularity was numerically similar between the two groups (Fig. 7). No significant differences were observed in the proportion and numbers of B cells, NK cells, neutrophils, and $CD11c^-$ F4/80-positive macrophages between the two groups of mice (data not shown). Overall these data suggest that the presence of T cells is associated with the development of overt pathology in the lungs of MHV-1-infected mice. Furthermore, the lungs of control mice have fewer alveolar macrophages. This might also influence local pathology and subsequent morbidity as alveolar macrophages are documented to modulate local inflammation by secreting immunosuppressive cytokines such as transforming growth factor β and IL-10 (62, 65).

Adoptive transfer of memory splenocytes into naïve hosts can contribute to morbidity and mortality following intranasal MHV-1 challenge. One of the cardinal features of the adaptive immune response is the development of immunological memory (2, 29, 64, 89). Memory T and B cells act as sentinels of the immune system and respond very rapidly to control a secondary infection in an effort to reduce morbidity (2, 29, 64, 89). Our T-cell depletion experiments showed that these cells exert a pathological effect following primary MHV-1 infection. In order to characterize their behavior following MHV-1 infection after their transition into memory cells, we adoptively transferred bulk memory splenocytes obtained from C3H/HeJ mice that had been infected more than 50 days previously into naïve recipients. The control group of mice received an equivalent number of splenocytes from naïve syngeneic donors. In addition, separate groups of recipient mice were injected with either purified memory CD4 T cells or CD8 T cells obtained from immune donors. The recipient mice were intranasally challenged with a sublethal dose of MHV-1 1 day after the adoptive transfer and were evaluated for weight loss and survival. All four groups of mice displayed signs and symptoms of disease, but whereas greater than 65% of the mice that received naïve splenocytes survived, only 29% of the mice that received bulk memory splenocytes recovered from the challenge (Fig. 8). None of the mice that received purified CD4 memory T cells survived the infectious challenge, while ~10% survival was observed in mice that received purified CD8 memory T cells (Fig. 7). The mortality rates in the recipients of the purified CD4 and CD8 memory T cells were not significantly different ($P > 0.05$) from each other as well as from mice that received bulk memory splenocytes, as determined by a Fisher's exact test. Data from preliminary studies comparing morbidity and mortality in MHV-1-infected memory cell-recipient mice revealed no significant differences between those that received bulk memory splenocytes and the mice that received CD19-depleted memory splenocytes, suggesting that T cells, and not B cells, were contributing to disease (data not shown). Taken together, our data suggest that repeat exposure to MHV-1 could be associated with an adverse outcome for a host unable to mount an effective neutralizing antibody response and therefore relying primarily on memory T-cell responses to

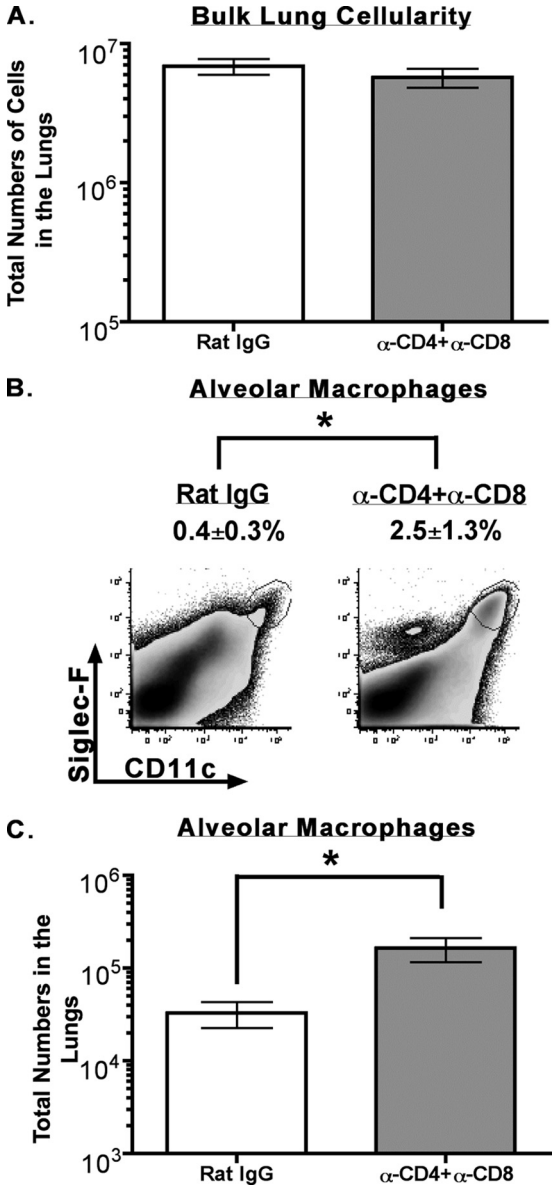

FIG. 7. Increased numbers of alveolar macrophages in the lungs of MHV-1-susceptible mice treated with T-cell-depleting antibodies. Lungs were harvested following perfusion from MHV-1-infected C3H/HeJ mice that were treated with either rat IgG or both anti-CD4 and anti-CD8 monoclonal antibodies as described in Materials and Methods. Single-cell suspensions were prepared, and bulk lung cells were counted using trypan blue exclusion (A). The single-cell suspensions were subsequently stained with a panel of monoclonal antibodies as described in Materials and Methods, examined by flow cytometry for the presence of alveolar macrophages ($CD11c^+$ Siglec-F^+), and enumerated by multiplying the percentage of $CD11c^+$ Siglec-F^+ cells by the numbers of cells measured in the bulk lung cell population (B and C). Results are representative of two experiments ($n = 3$ to 5 per group). Data are shown as means ± SEM, and statistically significant differences between control mice and mice treated with both anti-CD4 and anti-CD8 monoclonal antibodies were determined using an unpaired Student's t test and are indicated by an asterisk. α, anti.

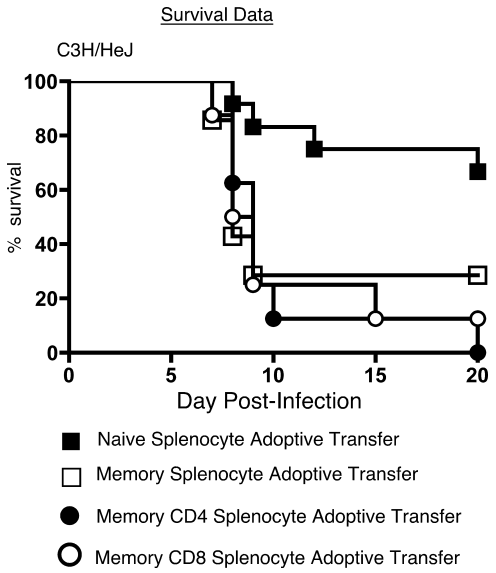

FIG. 8. Memory splenocytes induce enhanced morbidity and mortality following intranasal MHV-1 infection. Naïve C3H/HeJ hosts received 2×10^7 splenocytes/mouse by intravenous injection from either naïve C3H/HeJ donors (filled squares; $n = 12$) or C3H/HeJ mice that had been immunized with MHV-1 50 to 224 days previously (open squares; $n = 8$). The data shown for bulk naïve and memory splenocyte adoptive transfers are representative of three independent experiments. Additionally, separate groups of naïve recipients also received physiologically relevant input numbers of either purified bulk CD4 (4.3×10^6 cells/mouse; filled circles; $n = 8$) or bulk CD8 (1.8×10^6 cells/mouse; open circles; $n = 8$) T cells obtained from donor mice that had been immunized with MHV-1 >200 days previously. The following day the recipient mice were intranasally challenged with 5×10^3 PFU/mouse of MHV-1. Survival data for the four groups of mice are represented by Kaplan-Meier curves indicating the percentages of mice that survived the challenge.

combat the infection. Additionally, these data suggest that both CD4 and CD8 memory T cells are capable of inducing immunopathology in the context of MHV-1 infection.

DISCUSSION

Intranasal MHV-1 infection of susceptible strains of inbred mice, such as C3H/HeJ and A/J, has been described as a useful small-animal model to study SARS (11, 30). In this report we have utilized this model to define the role of the innate and adaptive components of the host immune response in the development of disease following intranasal MHV-1 infection. We find that C3H/HeJ mice rather than the A/J mice are the most susceptible to MHV-1-induced disease and that, as previously reported, B6 mice are the most resistant. Type I IFN-mediated signaling, NK cells, and the adaptive immune response play crucial roles in mediating protection in B6 mice following MHV-1 infection. In contrast to results obtained with the neurotropic JHM-MHV strain (3, 41, 50), a closely related group 2 CoV that preferentially infects the CNS instead of the lungs after intranasal infection, analysis of specific effector pathways employed by immune cells shows that the selective absence of perforin, IFN-γ, or TNF-α does not compromise the resistance of B6 mice to MHV-1-induced disease. However, the role of the immune response in the susceptible strains of mice appears to be complex. C3H/HeJ mice, despite being deficient in Toll-like receptor 4 (TLR4), can clear the virus but develop overt signs and symptoms of MHV-1-induced disease, including severe weight loss and increased Penh. This infection induces the development of an effective neutralizing antibody response in mice that survive as serum from previously immunized mice was able to effectively protect naïve hosts after exposure to MHV-1. Interestingly, short-term antibody-mediated depletion of T cells at and around the time of primary infection appears to markedly alleviate morbidity in the C3H/HeJ mice. Another notable finding of our study is that memory T cells appear to contribute considerably toward morbidity and mortality following intranasal MHV-1 infection in the absence of preformed antibody.

One of the findings of our study is that C3H/HeJ mice are more susceptible than A/J mice to MHV-1-induced disease. A previous report had shown that A/J mice were more susceptible to MHV-1-induced disease than C3H/St mice that displayed intermediate susceptibility (11). In our hands the viral dose required to establish a sublethal infection in A/J mice is 10^4 PFU/mouse. Infecting C3H/HeJ mice with this dose resulted in 80% mortality (data not shown), requiring us to scale down the amount of input virus to 5×10^3 PFU/mouse in C3H/HeJ mice. One of the reasons for the difference between our data and the earlier report could be the different susceptibilities of substrains of C3H mice used in the studies. De Albuquerque et al. (11) evaluated the effects of MHV-1 infection in C3H/St mice, whereas we utilized C3H/HeJ mice that are deficient in TLR4-mediated signaling (49). Similar substrain-specific differences in susceptibility to MHV-1-induced disease were also observed in our previous study that examined C3H/HeNCr mice that possess an intact TLR4-associated signaling pathway and are more resistant to MHV-1-induced disease than the C3H/HeJ mice (30).

Several reports have indicated that type I IFN responses play an important protective role in the context of CoV infections (9, 13, 17, 87). Antigen-presenting cells such as macrophages and conventional dendritic cells (DCs) are important targets of CoVs, and it has been suggested that plasmacytoid DC-derived type I IFN mediates initial control of viral replication in secondary lymphoid organs, thus allowing for the induction of successful adaptive immune responses that provide additional control of viral replication and limit systemic spread of infection (9, 55, 70, 88). Additionally, there are reports in the literature that show that type I IFNs provide a crucial third signal that induces the elaboration of optimal T-cell responses (33). Our data with MHV-1 confirm that an intact type I IFN pathway plays an important protective role as infection of B6 mice that lacked type I IFN-mediated signaling resulted in severe morbidity and rapid mortality. This outcome most likely resulted from an inability to efficiently induce IFN-stimulated genes including important antiviral molecules such as protein kinase RNA activated, RNase L, Mx, inducible nitric oxide synthase, and IFN-stimulated gene-15 (38, 39), leading to unrestrained replication in the respiratory tract and subsequent systemic spread.

NK cells constitute an important first line of defense in the host response against viral infections (27, 28, 44, 80, 81), and this response usually comes into play within 18 to 36 h following infection. Destruction of the infected target cells is medi-

ated by the release of effector molecules such as perforin, granzymes, and IFN-γ (27, 28, 44, 80, 81). There is published evidence to suggest that NK cells can modulate disease severity and survival in recombinant MHV (CXCL10-expressing strain A59)-infected Rag1-KO mice by controlling viral replication (69, 71). However, in JHM-MHV-infected mice that possess an intact immune system, NK cells are not critical for controlling viral clearance and disease (66, 67, 74). There is increasing evidence to suggest that optimal NK cell effector function is strongly influenced by type I IFN-mediated signaling (44). When DCs sense the presence of pathogens through pattern recognition receptors such as TLRs, they produce type I IFN which binds to type I IFN receptors on the surface of the DC itself, leading to the production and *trans*-presentation of IL-15 by the DCs to the NK cells that are then optimally primed to execute their effector functions (44). Based on this paradigm, we wondered if the rapid onset of morbidity and mortality and unrestrained viral replication in MHV-1-infected type I IFN-αβR-KO B6 mice was the result of a suboptimal NK cell response. However, our analysis of NK cell-depleted B6 mice revealed that although there was no difference in viral titers compared to wild-type controls, NK cell depletion resulted in increased morbidity, as evidenced by loss of body weight following infection. This finding is interesting, given that previously published reports indicate that the NK cell response in JHM-MHV-infected immunocompetent hosts does not impact the course of disease (66, 67, 74). An inability to see an increase in viral titers following NK cell depletion suggests either that the type I IFN response in itself is adequate to exert early control over viral replication or that it is possible that residual NK cells that persisted following antibody treatment (our antibody treatment resulted in 80% depletion of NK cells in the spleens) were sufficient to control the viral infection. The increased morbidity we observed in the NK cell-depleted infected mice might be the result of an increased inflow of neutrophils and macrophages into the lungs of these mice. It has been reported that macrophages are present in large numbers in the lungs of SARS-CoV-infected patients (55). Additionally, we have previously shown that macrophage infiltration is observed in the lungs of infected B6 mice (30). NK cell depletion might allow for a proportionally increased fraction of tissue damage-inducing macrophages to traffic into the lungs of MHV-1-infected B6 mice, thereby contributing to enhanced morbidity and mortality. Experiments are currently under way to examine these possibilities.

We also examined the role of specific effector molecules such as perforin, IFN-γ, or TNF-α in their ability to influence the outcome of MHV-1-induced disease in resistant B6 mice. It has been established that perforin and IFN-γ expressed by CD8 T cells are required to control virus replication and CNS disease after JHM-MHV infection of mice (3, 41, 50). However, our analysis revealed that the individual absence of perforin, IFN-γ, or TNF-α was not sufficient to suppress the resistance of B6 mice to MHV-1-induced disease after intranasal infection. These data suggest that at least in the context of MHV-1 infection, no single effector pathway seems to play a dominant role in controlling the course of disease.

CoV infection of mice results in the generation of neutralizing antibodies that are predominantly directed against the receptor-binding domain of the viral spike protein (4, 5, 6, 10, 14, 21, 43, 73, 79). Neutralizing antibodies are especially effective at preventing or minimizing infection of cells following reexposure to the pathogen (4, 5, 6, 10, 14, 21, 43, 73, 79). However, in the context of some CoVs, such as feline infectious peritonitis virus infection of previously immunized cats, and MHV-JHM infection of Rag1-KO mice, the presence of neutralizing antibodies induces opsonization of the virus particles, favoring uptake of these antigen-antibody complexes by Fc-receptor-bearing macrophages (12, 32, 55). This results in enhanced infection and subsequent activation of these cells, which then go on to mediate tissue destruction and worsen disease symptoms. However, data from SARS studies in mice demonstrate that antibodies generated following immunization with a DNA vaccine expressing the full-length spike protein of the human CoV-SARS Urbani strain effectively neutralized the 2002 and 2003 human SARS-CoV strains without enhancing infection (34, 79). Our data with MHV-1 demonstrate a similar protective effect of MHV-1-specific neutralizing antibodies when we challenged either C3H/HeJ or A/J mice that had been treated with immune serum obtained from previously immunized syngeneic donors. These results lend further support to the observation that MHV-1 infection of mice is a useful model to study SARS and have important implications for vaccine design to combat future SARS outbreaks.

Although there are a growing number of reports in the literature that have examined CD4 and CD8 T-cell responses following SARS-CoV infection in small-animal models and human subjects (15, 24, 25, 53, 54, 78, 85), there is no conclusive evidence to suggest that these responses actually contribute to immunopathology. However, there is evidence from studies involving MHV-JHM and MHV-A59 infections of Rag1-KO mice that implicate adoptively transferred CD4 and CD8 T cells as contributors to immunopathology in the CNS (23, 77). The T-cell responses elaborate a number of proinflammatory cytokines and chemokines that activate macrophages, which traffic into the brains of infected mice and induce myelin destruction. Accumulation of activated macrophages has also been reported in the lungs of SARS-CoV-infected patients (55). In order to directly ascertain the role of CD4 and CD8 T cells in the development of disease following intranasal MHV-1 infection, we resorted to antibody-mediated depletion of CD4 and CD8 T cells during the course of primary infection of susceptible A/J and C3H/HeJ mice. Depletion of both CD4 and CD8 T cells simultaneously resulted in a significant improvement in the disease severity and, specifically, airway function in the susceptible mice. Depleting only CD4 or CD8 T cells also improved the clinical outcome following infection, but the improvement was not as impressive as that observed when both subsets were depleted. Furthermore, the lungs of mice treated with both anti-CD4 and anti-CD8 monoclonal antibodies displayed significantly reduced alveolar fibrin deposition and edema formation and also had lower levels of IFN-γ, as measured by ELISA. These findings are suggestive of the fact that the presence of T cells is associated with the development of overt pathology in the lungs. Additionally, the lungs of mice treated with the T-cell-depleting antibodies had more alveolar macrophages than the lungs of control mice. Alveolar macrophages act as sentinels of the alveolar-blood interface, sensing the presence of pathogens

to secrete cytokines/chemokines that can recruit immune cells to initiate local inflammatory responses (62, 65). But the alveolar macrophages play an equally important role in resolving inflammation by phagocytosing apoptotic inflammatory cells and producing anti-inflammatory cytokines such as transforming growth factor β and IL-10 (62, 65). Collectively, these data suggest that both CD4 and CD8 T cells might be important contributors to the pathology observed in the lungs of infected animals.

One of the hallmarks of the adaptive immune response is the establishment of memory T and B cells that respond vigorously in the event of reexposure to the same pathogen (2, 29, 64, 89). This response is responsible for rapidly eliminating the pathogen and therefore potentially minimizing morbidity (2, 29, 64, 89). One of the most interesting findings of our study is that both memory CD4 and CD8 T-cell responses actually enhanced morbidity and mortality following MHV-1 rechallenge of C3H/HeJ mice in the absence of preformed antibody. Primary intranasal infection of naïve C3H/HeJ mice with a sublethal dose of MHV-1 induces robust antigen-specific CD4 and CD8 T-cell responses (unpublished observations). These antigen-specific CD4 and CD8 T cells are very efficient at producing IFN-γ as well as other proinflammatory cytokines. During a recall response that occurs in hosts lacking preformed neutralizing antibody (such as virally challenged naïve recipient mice adoptively transferred with memory splenocytes), it is very likely that the magnitude of the ensuing secondary T-cell response is much stronger than that observed during a primary response. This most likely plays an important role in the enhancement of morbidity and mortality we see in these mice. These data are also consistent with studies utilizing JHM strain of MHV that suggest that both CD4 and CD8 T cells can mediate CNS disease following infection.

Collectively, our data from primary MHV-1 infection studies in C3H/HeJ mice suggest that T-cell responses in MHV-1-susceptible strains contribute significantly to the severity of disease. Furthermore, their propensity to induce immunopathology is retained as these cells differentiate into memory cells, and their participation in recall responses amplifies their pathological behavior. Overall, these findings are compelling as they demonstrate T-cell-mediated immunopathology in CoV-infected mice that possess an intact T-cell compartment, and they corroborate previous data from T-cell adoptive transfer studies with MHV-JHM- and MHV-A59-infected Rag1-KO mice (23, 77).

In conclusion, in this study we have presented a detailed examination of the immune responses to MHV-1 following intranasal infection of susceptible and resistant strains of mice. Our analysis highlights the protective and pathological roles of the host immune response to MHV-1. These findings have important implications for the pathogenesis of SARS and offer insights into potential strategies that could be exploited for vaccine design. Future studies will focus on identifying MHV-1-specific CD4 and CD8 T cells and delineating effector pathways that could be involved in either mediating resistance or contributing to disease.

ACKNOWLEDGMENTS

We thank Stanley Perlman for critical review of the manuscript.

This work was supported by the National Institutes of Health Program Project grant PO1 AI-060699 (to J.T.H. and S.M.V.).

REFERENCES

1. **Badovinac, V. P., S. E. Hamilton, and J. T. Harty.** 2003. Viral infection results in massive $CD8^+$ T cell expansion and mortality in vaccinated perforin-deficient mice. Immunity **18:**463–474.
2. **Badovinac, V. P., and J. T. Harty.** 2006. Programming, demarcating, and manipulating $CD8^+$ T-cell memory. Immunol. Rev. **211:**67–80.
3. **Bergmann, C. C., B. Parra, D. R. Hinton, C. Ramakrishna, K. C. Dowdell, and S. A. Stohlman.** 2004. Perforin and gamma interferon-mediated control of coronavirus central nervous system infection by CD8 T cells in the absence of CD4 T cells. J. Virol. **78:**1739–1750.
4. **Bisht, H., A. Roberts, L. Vogel, A. Bukreyev, P. L. Collins, B. R. Murphy, K. Subbarao, and B. Moss.** 2004. Severe acute respiratory syndrome coronavirus spike protein expressed by attenuated vaccinia virus protectively immunizes mice. Proc. Natl. Acad. Sci. USA **101:**6641–6646.
5. **Buchholz, U. J., A. Bukreyev, L. Yang, E. W. Lamirande, B. R. Murphy, K. Subbarao, and P. L. Collins.** 2004. Contributions of the structural proteins of severe acute respiratory syndrome coronavirus to protective immunity. Proc. Natl. Acad. Sci. USA **101:**9804–9809.
6. **Bukreyev, A., E. W. Lamirande, U. J. Buchholz, L. N. Vogel, W. R. Elkins, M. St Claire, B. R. Murphy, K. Subbarao, and P. L. Collins.** 2004. Mucosal immunisation of African green monkeys (*Cercopithecus aethiops*) with an attenuated parainfluenza virus expressing the SARS coronavirus spike protein for the prevention of SARS. Lancet **363:**2122–2127.
7. **Burrows, P. D., and M. D. Cooper.** 1997. B cell development and differentiation. Curr. Opin. Immunol. **9:**239–244.
8. **Cameron, M. J., L. Ran, L. Xu, A. Danesh, J. F. Bermejo-Martin, C. M. Cameron, M. P. Muller, W. L. Gold, S. E. Richardson, S. M. Poutanen, B. M. Willey, M. E. DeVries, Y. Fang, C. Seneviratne, S. E. Bosinger, D. Persad, P. Wilkinson, L. D. Greller, R. Somogyi, A. Humar, S. Keshavjee, M. Louie, M. B. Loeb, J. Brunton, A. J. McGeer, and D. J. Kelvin.** 2007. Interferon-mediated immunopathological events are associated with atypical innate and adaptive immune responses in patients with severe acute respiratory syndrome. J. Virol. **81:**8692–8706.
9. **Cervantes-Barragan, L., R. Zust, F. Weber, M. Spiegel, K. S. Lang, S. Akira, V. Thiel, and B. Ludewig.** 2007. Control of coronavirus infection through plasmacytoid dendritic-cell-derived type I interferon. Blood **109:**1131–1137.
10. **Chen, Z., L. Zhang, C. Qin, L. Ba, C. E. Yi, F. Zhang, Q. Wei, T. He, W. Yu, J. Yu, H. Gao, X. Tu, A. Gettie, M. Farzan, K. Y. Yuen, and D. D. Ho.** 2005. Recombinant modified vaccinia virus Ankara expressing the spike glycoprotein of severe acute respiratory syndrome coronavirus induces protective neutralizing antibodies primarily targeting the receptor binding region. J. Virol. **79:**2678–2688.
11. **De Albuquerque, N., E. Baig, X. Ma, J. Zhang, W. He, A. Rowe, M. Habal, M. Liu, I. Shalev, G. P. Downey, R. Gorczynski, J. Butany, J. Leibowitz, S. R. Weiss, I. D. McGilvray, M. J. Phillips, E. N. Fish, and G. A. Levy.** 2006. Murine hepatitis virus strain 1 produces a clinically relevant model of severe acute respiratory syndrome in A/J. mice. J. Virol. **80:**10382–10394.
12. **de Groot, R. J., and M. C. Horzinek.** 1995. Feline infectious peritonitis, p. 293–315. *In* S. G. Siddell (ed.), The *Coronaviridae*. Plenum, New York, NY.
13. **de Lang, A., T. Baas, T. Teal, L. M. Leijten, B. Rain, A. D. Osterhaus, B. L. Haagmans, and M. G. Katze.** 2007. Functional genomics highlights differential induction of antiviral pathways in the lungs of SARS-CoV-infected macaques. PLoS Pathog. **3:**e112.
14. **Du, L., Y. He, Y. Wang, H. Zhang, S. Ma, C. K. Wong, S. H. Wu, F. Ng, J. D. Huang, K. Y. Yuen, S. Jiang, Y. Zhou, and B. J. Zheng.** 2006. Recombinant adeno-associated virus expressing the receptor-binding domain of severe acute respiratory syndrome coronavirus S protein elicits neutralizing antibodies: Implication for developing SARS vaccines. Virology **353:**6–16.
15. **Du, L., G. Zhao, Y. Lin, H. Sui, C. Chan, S. Ma, Y. He, S. Jiang, C. Wu, K. Y. Yuen, D. Y. Jin, Y. Zhou, and B. J. Zheng.** 2008. Intranasal vaccination of recombinant adeno-associated virus encoding receptor-binding domain of severe acute respiratory syndrome coronavirus (SARS-CoV) spike protein induces strong mucosal immune responses and provides long-term protection against SARS-CoV infection. J. Immunol. **180:**948–956.
16. **Fouchier, R. A., T. Kuiken, M. Schutten, G. van Amerongen, G. J. van Doornum, B. G. van den Hoogen, M. Peiris, W. Lim, K. Stohr, and A. D. Osterhaus.** 2003. Aetiology: Koch's postulates fulfilled for SARS virus. Nature **423:**240.
17. **Frieman, M., B. Yount, M. Heise, S. A. Kopecky-Bromberg, P. Palese, and R. S. Baric.** 2007. Severe acute respiratory syndrome coronavirus ORF6 antagonizes STAT1 function by sequestering nuclear import factors on the rough endoplasmic reticulum/Golgi membrane. J. Virol. **81:**9812–9824.
18. **Gallagher, T. M.** 1996. Murine coronavirus membrane fusion is blocked by modification of thiols buried within the spike protein. J. Virol. **70:**4683–4690.
19. **Guidotti, L. G., and F. V. Chisari.** 2001. Noncytolytic control of viral infections by the innate and adaptive immune response. Annu. Rev. Immunol. **19:**65–91.
20. **Harty, J. T., A. R. Tvinnereim, and D. W. White.** 2000. $CD8^+$ T cell effector mechanisms in resistance to infection. Annu. Rev. Immunol. **18:**275–308.

21. **He, Y., J. Li, S. Heck, S. Lustigman, and S. Jiang.** 2006. Antigenic and immunogenic characterization of recombinant baculovirus-expressed severe acute respiratory syndrome coronavirus spike protein: implication for vaccine design. J. Virol. **80:**5757–5767.
22. **Holmes, K. V.** 2003. SARS-associated coronavirus. N. Engl. J. Med. **348:** 1948–1951.
23. **Houtman, J. J., and J. O. Fleming.** 1996. Dissociation of demyelination and viral clearance in congenitally immunodeficient mice infected with murine coronavirus JHM. J. Neurovirol. **2:**101–110.
24. **Huang, J., Y. Cao, J. Du, X. Bu, R. Ma, and C. Wu.** 2007. Priming with SARS CoV S DNA and boosting with SARS CoV S epitopes specific for $CD4^+$ and $CD8^+$ T cells promote cellular immune responses. Vaccine **25:**6981–6991.
25. **Huang, J., R. Ma, and C. Y. Wu.** 2006. Immunization with SARS-CoV S DNA vaccine generates memory $CD4^+$ and $CD8^+$ T cell immune responses. Vaccine **24:**4905–4913.
26. **Jones, B. M., E. S. Ma, J. S. Peiris, P. C. Wong, J. C. Ho, B. Lam, K. N. Lai, and K. W. Tsang.** 2004. Prolonged disturbances of in vitro cytokine production in patients with severe acute respiratory syndrome (SARS) treated with ribavirin and steroids. Clin. Exp. Immunol. **135:**467–473.
27. **Karre, K.** 1995. Express yourself or die: peptides, MHC molecules, and NK cells. Science **267:**978–979.
28. **Karre, K.** 2008. Natural killer cell recognition of missing self. Nat. Immunol. **9:**477–480.
29. **Khanolkar, A., V. P. Badovinac, and J. T. Harty.** 2007. CD8 T cell memory development: CD4 T cell help is appreciated. Immunol. Res. **39:**94–104.
30. **Khanolkar, A., S. M. Hartwig, B. A. Haag, D. K. Meyerholz, J. T. Harty, and S. M. Varga.** 24 June 2009. TLR4 deficiency increases disease and mortality after mouse hepatitis virus type 1 infection in susceptible C3H mice. J. Virol. doi:10.1128/JVI.01857-08.
31. **Khanolkar, A., M. J. Fuller, and A. J. Zajac.** 2002. T cell responses to viral infections: lessons from lymphocytic choriomeningitis virus. Immunol. Res. **26:**309–321.
32. **Kim, T. S., and S. Perlman.** 2005. Virus-specific antibody, in the absence of T cells, mediates demyelination in mice infected with a neurotropic coronavirus. Am. J. Pathol. **166:**801–809.
33. **Kolumam, G. A., S. Thomas, L. J. Thompson, J. Sprent, and K. Murali-Krishna.** 2005. Type I interferons act directly on CD8 T cells to allow clonal expansion and memory formation in response to viral infection. J. Exp. Med. **202:**637–650.
34. **Kong, W. P., L. Xu, K. Stadler, J. B. Ulmer, S. Abrignani, R. Rappuoli, and G. J. Nabel.** 2005. Modulation of the immune response to the severe acute respiratory syndrome spike glycoprotein by gene-based and inactivated virus immunization. J. Virol. **79:**13915–13923.
35. **Ksiazek, T. G., D. Erdman, C. S. Goldsmith, S. R. Zaki, T. Peret, S. Emery, S. Tong, C. Urbani, J. A. Comer, W. Lim, P. E. Rollin, S. F. Dowell, A. E. Ling, C. D. Humphrey, W. J. Shieh, J. Guarner, C. D. Paddock, P. Rota, B. Fields, J. DeRisi, J. Y. Yang, N. Cox, J. M. Hughes, J. W. LeDuc, W. J. Bellini, and L. J. Anderson.** 2003. A novel coronavirus associated with severe acute respiratory syndrome. N. Engl. J. Med. **348:**1953–1966.
36. **La Gruta, N. L., K. Kedzierska, J. Stambas, and P. C. Doherty.** 2007. A question of self-preservation: immunopathology in influenza virus infection. Immunol. Cell Biol. **85:**85–92.
37. **Lee, N., D. Hui, A. Wu, P. Chan, P. Cameron, G. M. Joynt, A. Ahuja, M. Y. Yung, C. B. Leung, K. F. To, S. F. Lui, C. C. Szeto, S. Chung, and J. J. Sung.** 2003. A major outbreak of severe acute respiratory syndrome in Hong Kong. N. Engl. J. Med. **348:**1986–1994.
38. **Lenschow, D. J., N. V. Giannakopoulos, L. J. Gunn, C. Johnston, A. K. O'Guin, R. E. Schmidt, B. Levine, and H. W. Virgin IV.** 2005. Identification of interferon-stimulated gene 15 as an antiviral molecule during Sindbis virus infection in vivo. J. Virol. **79:**13974–13983.
39. **Lenschow, D. J., C. Lai, N. Frias-Staheli, N. V. Giannakopoulos, A. Lutz, T. Wolff, A. Osiak, B. Levine, R. E. Schmidt, A. Garcia-Sastre, D. A. Leib, A. Pekosz, K. P. Knobeloch, I. Horak, and H. W. Virgin IV.** 2007. IFN-stimulated gene 15 functions as a critical antiviral molecule against influenza, herpes, and Sindbis viruses. Proc. Natl. Acad. Sci. USA **104:**1371–1376.
40. **Li, W., Z. Shi, M. Yu, W. Ren, C. Smith, J. H. Epstein, H. Wang, G. Crameri, Z. Hu, H. Zhang, J. Zhang, J. McEachern, H. Field, P. Daszak, B. T. Eaton, S. Zhang, and L. F. Wang.** 2005. Bats are natural reservoirs of SARS-like coronaviruses. Science **310:**676–679.
41. **Lin, M. T., S. A. Stohlman, and D. R. Hinton.** 1997. Mouse hepatitis virus is cleared from the central nervous systems of mice lacking perforin-mediated cytolysis. J. Virol. **71:**383–391.
42. **Loutfy, M. R., L. M. Blatt, K. A. Siminovitch, S. Ward, B. Wolff, H. Lho, D. H. Pham, H. Deif, E. A. LaMere, M. Chang, K. C. Kain, G. A. Farcas, P. Ferguson, M. Latchford, G. Levy, J. W. Dennis, E. K. Lai, and E. N. Fish.** 2003. Interferon alfacon-1 plus corticosteroids in severe acute respiratory syndrome: a preliminary study. JAMA **290:**3222–3228.
43. **Lu, X., Y. Chen, B. Bai, H. Hu, L. Tao, J. Yang, J. Chen, Z. Chen, Z. Hu, and H. Wang.** 2007. Immune responses against severe acute respiratory syndrome coronavirus induced by virus-like particles in mice. Immunology **122:** 496–502.
44. **Lucas, M., W. Schachterle, K. Oberle, P. Aichele, and A. Diefenbach.** 2007. Dendritic cells prime natural killer cells by trans-presenting interleukin 15. Immunity **26:**503–517.
45. **Marra, M. A., S. J. Jones, C. R. Astell, R. A. Holt, A. Brooks-Wilson, Y. S. Butterfield, J. Khattra, J. K. Asano, S. A. Barber, S. Y. Chan, A. Cloutier, S. M. Coughlin, D. Freeman, N. Girn, O. L. Griffith, S. R. Leach, M. Mayo, H. McDonald, S. B. Montgomery, P. K. Pandoh, A. S. Petrescu, A. G. Robertson, J. E. Schein, A. Siddiqui, D. E. Smailus, J. M. Stott, G. S. Yang, F. Plummer, A. Andonov, H. Artsob, N. Bastien, K. Bernard, T. F. Booth, D. Bowness, M. Czub, M. Drebot, L. Fernando, R. Flick, M. Garbutt, M. Gray, A. Grolla, S. Jones, H. Feldmann, A. Meyers, A. Kabani, Y. Li, S. Normand, U. Stroher, G. A. Tipples, S. Tyler, R. Vogrig, D. Ward, B. Watson, R. C. Brunham, M. Krajden, M. Petric, D. M. Skowronski, C. Upton, and R. L. Roper.** 2003. The Genome sequence of the SARS-associated coronavirus. Science **300:**1399–1404.
46. **Mombaerts, P., J. Iacomini, R. S. Johnson, K. Herrup, S. Tonegawa, and V. E. Papaioannou.** 1992. RAG-1-deficient mice have no mature B and T lymphocytes. Cell **68:**869–877.
47. **Muller, U., U. Steinhoff, L. F. Reis, S. Hemmi, J. Pavlovic, R. M. Zinkernagel, and M. Aguet.** 1994. Functional role of type I and type II interferons in antiviral defense. Science **264:**1918–1921.
48. **Nagata, N., N. Iwata, H. Hasegawa, S. Fukushi, A. Harashima, Y. Sato, M. Saijo, F. Taguchi, S. Morikawa, and T. Sata.** 2008. Mouse-passaged severe acute respiratory syndrome-associated coronavirus leads to lethal pulmonary edema and diffuse alveolar damage in adult but not young mice. Am. J. Pathol. **172:**1625–1637.
49. **Outzen, H. C., D. Corrow, and L. D. Shultz.** 1985. Attenuation of exogenous murine mammary tumor virus virulence in the C3H/HeJ mouse substrain bearing the Lps mutation. J. Natl. Cancer Inst. **75:**917–923.
50. **Parra, B., D. R. Hinton, N. W. Marten, C. C. Bergmann, M. T. Lin, C. S. Yang, and S. A. Stohlman.** 1999. IFN-gamma is required for viral clearance from central nervous system oligodendroglia. J. Immunol. **162:**1641–1647.
51. **Pasparakis, M., L. Alexopoulou, M. Grell, K. Pfizenmaier, H. Bluethmann, and G. Kollias.** 1997. Peyer's patch organogenesis is intact yet formation of B lymphocyte follicles is defective in peripheral lymphoid organs of mice deficient for tumor necrosis factor and its 55-kDa receptor. Proc. Natl. Acad. Sci. USA **94:**6319–6323.
52. **Peiris, J. S., Y. Guan, and K. Y. Yuen.** 2004. Severe acute respiratory syndrome. Nat. Med. **10:**S88–97.
53. **Peng, H., L. T. Yang, J. Li, Z. Q. Lu, L. Y. Wang, R. A. Koup, R. T. Bailer, and C. Y. Wu.** 2006. Human memory T cell responses to SARS-CoV E protein. Microbes Infect. **8:**2424–2431.
54. **Peng, H., L. T. Yang, L. Y. Wang, J. Li, J. Huang, Z. Q. Lu, R. A. Koup, R. T. Bailer, and C. Y. Wu.** 2006. Long-lived memory T lymphocyte responses against SARS coronavirus nucleocapsid protein in SARS-recovered patients. Virology **351:**466–475.
55. **Perlman, S., and A. A. Dandekar.** 2005. Immunopathogenesis of coronavirus infections: implications for SARS. Nat. Rev. Immunol. **5:**917–927.
56. **Perlman, S., R. Schelper, E. Bolger, and D. Ries.** 1987. Late onset, symptomatic, demyelinating encephalomyelitis in mice infected with MHV-JHM in the presence of maternal antibody. Microb. Pathog. **2:**185–194.
57. **Poutanen, S. M., D. E. Low, B. Henry, S. Finkelstein, D. Rose, K. Green, R. Tellier, R. Draker, D. Adachi, M. Ayers, A. K. Chan, D. M. Skowronski, I. Salit, A. E. Simor, A. S. Slutsky, P. W. Doyle, M. Krajden, M. Petric, R. C. Brunham, and A. J. McGeer.** 2003. Identification of severe acute respiratory syndrome in Canada. N. Engl. J. Med. **348:**1995–2005.
58. **Reghunathan, R., M. Jayapal, L. Y. Hsu, H. H. Chng, D. Tai, B. P. Leung, and A. J. Melendez.** 2005. Expression profile of immune response genes in patients with severe acute respiratory syndrome. BMC Immunol. **6:**2.
59. **Roberts, A., D. Deming, C. D. Paddock, A. Cheng, B. Yount, L. Vogel, B. D. Herman, T. Sheahan, M. Heise, G. L. Genrich, S. R. Zaki, R. Baric, and K. Subbarao.** 2007. A mouse-adapted SARS-coronavirus causes disease and mortality in BALB/c mice. PLoS Pathog. **3:**e5.
60. **Roberts, A., E. W. Lamirande, L. Vogel, J. P. Jackson, C. D. Paddock, J. Guarner, S. R. Zaki, T. Sheahan, R. Baric, and K. Subbarao.** 2008. Animal models and vaccines for SARS-CoV infection. Virus Res. **133:**20–32.
61. **Rota, P. A., M. S. Oberste, S. S. Monroe, W. A. Nix, R. Campagnoli, J. P. Icenogle, S. Penaranda, B. Bankamp, K. Maher, M. H. Chen, S. Tong, A. Tamin, L. Lowe, M. Frace, J. L. DeRisi, Q. Chen, D. Wang, D. D. Erdman, T. C. Peret, C. Burns, T. G. Ksiazek, P. E. Rollin, A. Sanchez, S. Liffick, B. Holloway, J. Limor, K. McCaustland, M. Olsen-Rasmussen, R. Fouchier, S. Gunther, A. D. Osterhaus, C. Drosten, M. A. Pallansch, L. J. Anderson, and W. J. Bellini.** 2003. Characterization of a novel coronavirus associated with severe acute respiratory syndrome. Science **300:**1394–1399.
62. **Rubins, J. B.** 2003. Alveolar macrophages: wielding the double-edged sword of inflammation. Am. J. Respir. Crit. Care Med. **167:**103–104.
63. **Snijder, E. J., P. J. Bredenbeek, J. C. Dobbe, V. Thiel, J. Ziebuhr, L. L. Poon, Y. Guan, M. Rozanov, W. J. Spaan, and A. E. Gorbalenya.** 2003. Unique and conserved features of genome and proteome of SARS-coronavirus, an early split-off from the coronavirus group 2 lineage. J. Mol. Biol. **331:**991–1004.
64. **Sprent, J., and C. D. Surh.** 2002. T cell memory. Annu. Rev. Immunol. **20:**551–579.
65. **Stevens, W. W., T. S. Kim, L. M. Pujanauski, X. Hao, and T. J. Braciale.**

2007. Detection and quantitation of eosinophils in the murine respiratory tract by flow cytometry. J. Immunol. Methods. **327:**63–74.
66. **Stohlman, S. A., C. C. Bergmann, and S. Perlman.** 1999. Mouse hepatitis virus, p. 537–557. *In* R. Ahmed and I. S. Y. Chen (ed.), Persistent viral infections. John Wiley and Sons Ltd., Chichester, United Kingdom.
67. **Stohlman, S. A., P. R. Brayton, R. C. Harmon, D. Stevenson, R. G. Ganges, and G. K. Matsushima.** 1983. Natural killer cell activity during mouse hepatitis virus infection: response in the absence of interferon. Int. J. Cancer. **31:**309–314.
68. **Thiel, V., K. A. Ivanov, A. Putics, T. Hertzig, B. Schelle, S. Bayer, B. Weissbrich, E. J. Snijder, H. Rabenau, H. W. Doerr, A. E. Gorbalenya, and J. Ziebuhr.** 2003. Mechanisms and enzymes involved in SARS coronavirus genome expression. J. Gen. Virol. **84:**2305–2315.
69. **Trifilo, M. J., C. Montalto-Morrison, L. N. Stiles, K. R. Hurst, J. L. Hardison, J. E. Manning, P. S. Masters, and T. E. Lane.** 2004. CXC chemokine ligand 10 controls viral infection in the central nervous system: evidence for a role in innate immune response through recruitment and activation of natural killer cells. J. Virol. **78:**585–594.
70. **Turner, B. C., E. M. Hemmila, N. Beauchemin, and K. V. Holmes.** 2004. Receptor-dependent coronavirus infection of dendritic cells. J. Virol. **78:** 5486–5490.
71. **Walsh, K. B., M. B. Lodoen, R. A. Edwards, L. L. Lanier, and T. E. Lane.** 2008. Evidence for differential roles for NKG2D receptor signaling in innate host defense against coronavirus-induced neurological and liver disease. J. Virol. **82:**3021–3030.
72. **Wang, W. K., S. Y. Chen, I. J. Liu, C. L. Kao, H. L. Chen, B. L. Chiang, J. T. Wang, W. H. Sheng, P. R. Hsueh, C. F. Yang, P. C. Yang, and S. C. Chang.** 2004. Temporal relationship of viral load, ribavirin, interleukin (IL)-6, IL-8, and clinical progression in patients with severe acute respiratory syndrome. Clin. Infect. Dis. **39:**1071–1075.
73. **Wang, X., W. Xu, D. Tong, J. Ni, H. Gao, Y. Wang, Y. Chu, P. Li, X. Yang, and S. Xiong.** 2008. A chimeric multi-epitope DNA vaccine elicited specific antibody response against severe acute respiratory syndrome-associated coronavirus which attenuated the virulence of SARS-CoV in vitro. Immunol. Lett. **119:**71–77.
74. **Williamson, J. S., K. C. Sykes, and S. A. Stohlman.** 1991. Characterization of brain-infiltrating mononuclear cells during infection with mouse hepatitis virus strain JHM. J. Neuroimmunol. **32:**199–207.
75. **Wong, C. K., C. W. Lam, A. K. Wu, W. K. Ip, N. L. Lee, I. H. Chan, L. C. Lit, D. S. Hui, M. H. Chan, S. S. Chung, and J. J. Sung.** 2004. Plasma inflammatory cytokines and chemokines in severe acute respiratory syndrome. Clin. Exp. Immunol. **136:**95–103.
76. **World Health Organization Multicentre Collaborative Network for Sever Acute Respiratory Syndrome Diagnosis.** 2003. A multicentre collaboration to investigate the cause of severe acute respiratory syndrome. Lancet **361:** 1730–1733.
77. **Wu, G. F., A. A. Dandekar, L. Pewe, and S. Perlman.** 2000. CD4 and CD8 T cells have redundant but not identical roles in virus-induced demyelination. J. Immunol. **165:**2278–2286.
78. **Yang, L. T., H. Peng, Z. L. Zhu, G. Li, Z. T. Huang, Z. X. Zhao, R. A. Koup, R. T. Bailer, and C. Y. Wu.** 2006. Long-lived effector/central memory T-cell responses to severe acute respiratory syndrome coronavirus (SARS-CoV) S antigen in recovered SARS patients. Clin. Immunol. **120:**171–178.
79. **Yang, Z. Y., W. P. Kong, Y. Huang, A. Roberts, B. R. Murphy, K. Subbarao, and G. J. Nabel.** 2004. A DNA vaccine induces SARS coronavirus neutralization and protective immunity in mice. Nature **428:**561–564.
80. **Yokoyama, W. M.** 2005. Natural killer cell immune responses. Immunol. Res. **32:**317–325.
81. **Yokoyama, W. M.** 2005. Specific and non-specific natural killer cell responses to viral infection. Adv. Exp. Med. Biol. **560:**57–61.
82. **Yu, S. Y., Y. W. Hu, X. Y. Liu, W. Xiong, Z. T. Zhou, and Z. H. Yuan.** 2005. Gene expression profiles in peripheral blood mononuclear cells of SARS patients. World J. Gastroenterol. **11:**5037–5043.
83. **Zhang, Y., J. Li, Y. Zhan, L. Wu, X. Yu, W. Zhang, L. Ye, S. Xu, R. Sun, Y. Wang, and J. Lou.** 2004. Analysis of serum cytokines in patients with severe acute respiratory syndrome. Infect. Immun. **72:**4410–4415.
84. **Zhao, Z., F. Zhang, M. Xu, K. Huang, W. Zhong, W. Cai, Z. Yin, S. Huang, Z. Deng, M. Wei, J. Xiong, and P. M. Hawkey.** 2003. Description and clinical treatment of an early outbreak of severe acute respiratory syndrome (SARS) in Guangzhou, PR China. J. Med. Microbiol. **52:**715–720.
85. **Zhi, Y., G. P. Kobinger, H. Jordan, K. Suchma, S. R. Weiss, H. Shen, G. Schumer, G. Gao, J. L. Boyer, R. G. Crystal, and J. M. Wilson.** 2005. Identification of murine CD8 T cell epitopes in codon-optimized SARS-associated coronavirus spike protein. Virology **335:**34–45.
86. **Zhong, N. S., B. J. Zheng, Y. M. Li, Poon, Z. H. Xie, K. H. Chan, P. H. Li, S. Y. Tan, Q. Chang, J. P. Xie, X. Q. Liu, J. Xu, D. X. Li, K. Y. Yuen, Peiris, and Y. Guan.** 2003. Epidemiology and cause of severe acute respiratory syndrome (SARS) in Guangdong, People's Republic of China, in February, 2003. Lancet **362:**1353–1358.
87. **Zhou, H., and S. Perlman.** 2007. Mouse hepatitis virus does not induce Beta interferon synthesis and does not inhibit its induction by double-stranded RNA. J. Virol. **81:**568–574.
88. **Zhou, H., and S. Perlman.** 2006. Preferential infection of mature dendritic cells by mouse hepatitis virus strain JHM. J. Virol. **80:**2506–2514.
89. **Zinkernagel, R. M.** 2002. On differences between immunity and immunological memory. Curr. Opin. Immunol. **14:**523–536.